

Fabrication of Porous β -Type Ti-40Nb Alloys Incorporated with TiH_2 via Powder Metallurgy Processing Route Under Reducing Environment

Siti Mariana Hosnie

Muhammad Hussain Ismail

Centre for Advanced Materials Research (CAMAR), Faculty of Mechanical Engineering, Universiti Teknologi MARA, 40450, Shah Alam, Malaysia

Mazyan Yahaya

Mechanical Engineering Department, Politeknik Sultan Salahuddin Abdul Aziz Shah, 40150, Shah Alam, Selangor, Malaysia

Nurul 'Ain binti Haris

Faculty of Mechanical Engineering, Universiti Teknologi MARA Campus Pasir Gudang Campus, 81750, Masai, Johor, Malaysia

Iain Todd

Innovative Materials Processing Centre (IMPC), Department of Materials Science and Engineering, The University of Sheffield, Sir Robert Hadfield Building, Mappin Street, Sheffield, S10 3JD, United Kingdom

ABSTRACT

This work attempts to investigate the influence of TiH_2 and processing route on microstructure and mechanical properties of Ti-40Nb alloy. The difference in processing route resulted in various microstructure constituent of β -phase as well as the mechanical properties of the alloy. These differences were beneficial towards the biomedical research to fit with the variability mechanical properties of human bone. The formation of porous and β -rich phase of TiNb was believed to help in lowering the Young's modulus value that subsequently alleviates the mismatch problem between the implant and human bones. Therefore, this work attempted to synthesize porous and β -phase TiNb alloy via powder metallurgy processing route under inert gas of argon associated with reducing environment of CaH_2 as the wicking agent. This route was chosen with the purpose to other processing routes such as Selective Laser Melting (SLM), hot pressing and

arc melting techniques. The raw materials with 40 wt% of Nb and 60 wt% of TiH₂ composition were mixed, compacted and sintered at 1200 °C using a tube furnace. The result showed that Ti-40Nb alloy with β - rich phase demonstrated a promising low Young's modulus for about 17 GPa, the compressive strength of 300MPa and porosity of 55% respectively. These results were compared with other processing route results for determination of better established method for Ti-40Nb alloy. An alternative route in processing Ti-40Nb alloy has been successfully demonstrated using low-cost techniques. The use of TiH₂ in reducing environment can reduce the problem of impurity uptake, particularly during sintering process.

Keywords: *Ti-Nb Alloy, Titanium Hydride, Powder Metallurgy, Dehydrogenation, Microstructure, Mechanical Properties.*

Introduction

In biomedical implant research, Ti alloy has been established as a well-known metallic material for implanting material due to the promising mechanical properties, high resistance to corrosion and the most important features is its level of biocompatible in the human body [1]–[3]. The usage of Ti alloy, particularly, Ti-6Al-4V has been commercialized in the implant markets [4]. However, the perception of Ti-6Al-4V as implant material has changed due to cytotoxic effect of Al and V [5]. The Vanadium has been detected to react severely with tissue in rabbit while the Al may be related to neurological disorders and the worst case is Alzheimer's disease [6]. Thus, the development of Ti-based alloy for implant material, now, has been focusing more on choosing an alloying element for Ti-alloy that is biocompatible in the human body; for instance Nb and Ta [7].

On the other side, recent research attempted in reducing Young's modulus by introducing porous structure and β -rich phase [8]–[10]. An effort for reducing the Young's modulus is owing to alleviate the stress shielding effect caused by a mismatch of the Young's modulus between the implant and human bones [7], [11]. The porous structure exhibits unique feature which does not only help in reducing the Young's modulus but also provide space for bone tissue ingrowth and thus promoting better fixation of the implant with the surrounding bone. Research conducted by Zhuravleva et al. (2013) [12] demonstrated that Young's modulus of β -TiNb exhibited compatible result with human cancellous bone (~3GPa) which is approximately 1.5 to 3GPa. The low value of Young's modulus is owing to the porous and β -rich phase of the TiNb alloy existence at the end of the reaction. Hence, the recent study on biomaterial implant is aimed to fabricate TiNb alloy which is porous in structure and contains β -rich phase using an

alternative route of powder metallurgy (PM) employing TiH₂ powder associated with reduced environment. The combination of porous structure and β -rich phase helps in reducing the Young's modulus value which mimics human bones of Young's modulus value respectively.

In the work patented by Davidson and Kovacs in 1992, the range of Nb content between 35-50 by mass fraction has been identified as significant in lowering the Young's modulus [13]. Another research conducted by Hon et al. [14] and Zhuravleva et al. [12] claimed that Ti-40Nb alloy had promising result in terms of microstructure and mechanical properties that were able to attain prototype for the implant material. Based on the literature, the TiNb alloy was successfully synthesized via arc melting [14], selective laser melting (SLM) [15], hot pressing [15] and powder metallurgy (PM) [14] processing routes which finally resulted in the final part with different properties. The mechanical properties were significantly influenced by the phase present, microstructure evolved and level of porosity.

Concerned with high manufacturing cost of the metallic implant, the current research is aimed to manufacture low-cost processing route. Among the metallic processing route, PM processing route has been identified as the best approach particularly to indicate shape with high volume production and to produce near-net-shape product [16]. An alternative approach to lowering the cost of production has been introduced by employing TiH₂ powder as the raw material instead of Ti powder. The manufacturing cost of using TiH₂ powder is lower rather than Ti powder. In the previous research, it had been shown that the cost by conventional route when using TiH₂ powder had been nine times smaller instead of using Ti powder as the raw material [17]. Another factor in Ti processing is the formation of carbide phase resulting from machining process [18]. PM techniques significantly reduce secondary operation by means of machining. Therefore, microstructure homogeneity can be maintained throughout the process [19].

The development of metallic implant in the above has been progressively researched. For metallic implant, for instance, many have focused on the porous structure in order to get the Young's modulus close to the human bone. The human bones have relatively different mechanical properties as related to the age as well as the type of the human bone such as cortical bone (10 to 30 GPa) and cancellous bone (~3GPa). Both bones have a different value of Young's modulus, respectively. Burstein et al. (1976) had reported that the mechanical properties of human bones with age-related roughly showed that the elastic modulus of the younger group has a significantly higher number rather than an older group [20]. For instance, the fibula of younger group had an elastic modulus of 19.2 GPa while the older group, 15.2 GPa, respectively. Table 1 shows an example of the compressive properties of human cortical bone. Even though, there was already established Ti-40Nb alloy research, the current work attempts on fabricating

Ti-40Nb alloy using an alternative approach to cope with the variability of human bone properties. The low-cost production by PM processing route as compared to another route, would expect to produce a new promising Ti-40Nb alloy for implant material. The results regarding the aspects of porous and β -phase which significantly influences the mechanical properties of TiNb alloy are discussed in this work. On the other hand, the porosity and mechanical properties are also compared with other processing route in order to establish a promising processing route that would be employed for fabrication implant material in the future.

Table 1: The variability compressive properties of the human cortical bone with different type of hard tissues [20]

Type of hard tissue	Age	Ultimate strength (MPa)	Elastic modulus (GPa)	Hardness (MPa)
Tibia osteons	57-61	-	22.5	614
Femur	20-89	194	17.6	-
Tibia	30-89	195	28.0	-

Experimental

Elemental TiH₂ powders (average particle size of 53 μ m) with a composition of 60 wt% and 40 wt% of Nb powder (average particle size of 130 μ m) were employed in this work. To have a homogenous mixture, the TiH₂ and Nb powders were mixed using a planetary ball mill Retsch PM 400. The powders were milled for 5 hours within 15 minutes interval with 12 repetitions at 200 rpm. After that, the mixed powder was pressed to form a green compact. The powders were consolidated at room temperature for uniaxially die-compacted using a force of 1000kg with a die cylindrical of 25mm in diameter. Then, the green compact samples were covered by CaH₂ powder for about 100-200 mg and placed in a tube furnace for sintering process. The samples were sintered at 1200°C and soaked for 2 hours under argon environment. Figure 1 shows the process in PM processing route employed in this work.

For analysis purpose, the sintered samples were cut using the electro-discharge machine (EDM). The as-sintered sample was subsequently cut into rectangular shape with a dimension of 4x4x8 mm³ in size for compression test purpose [10]. The cut sample was then slightly polished using 320 grit paper in order to remove any oxidized surface that probably formed from the cutting process. The oxidized surface needs to be removed due to its properties that might affect the mechanical properties of TiNb alloy. The mechanical properties of TiNb alloy were investigated by uniaxial compression test using Instron 3382 universal machine. The test was

performed at ambient temperature using cylindrical cage insuring parallelism which contained a screw-driven load frame.

The metallographic analysis of the prepared samples was examined after undergoing metallographically grind and polish. The sample was mounted in epoxy resin and subsequently grounded using 120, 320, 600 and 1200-SiC papers respectively. The grinding process was followed by a polish process using 6 μ , 3 μ , and 1 μ of the diamond slurry. The microstructural analysis was examined using a Hitachi Scanning Electron Microscopy (SEM) under the Secondary Electron Imaging and Back-Scattered Imaging.

The phase for the as-sintered sample was characterized by X-ray diffraction analysis (XRD) using a Rigaku 3014, Japan with Cu K α radiation 1.54Å under 40kV and 40mA. The diffraction intensity was recorded between 30° to 90° with a scanning rate of 0.03°s⁻¹. The XRD patterns for TiNb alloy was studied based on JCPD.

The porosity (P) of TiNb alloy was calculated by using Equation (1) as shown below:

$$P = 1 - \frac{\rho}{\rho_s} 100\% \quad (1)$$

Where ρ is the density of TiNb alloy which is determined by the geometrical method. The porosity of the alloy was measured using at least three sintered samples with a deviation of $\pm 1.5\%$. Meanwhile, ρ_0 is the theoretical density which is calculated using rule of mixture as shown in Equation (2):

$$\rho_0 = \frac{1}{(A\% / \rho_A) + (B\% / \rho_B)} \quad (2)$$

Where A% and B% are the weight fraction of TiH₂ and Nb powders respectively while ρ_A and ρ_B are the theoretical density of TiH₂ and Nb respectively.

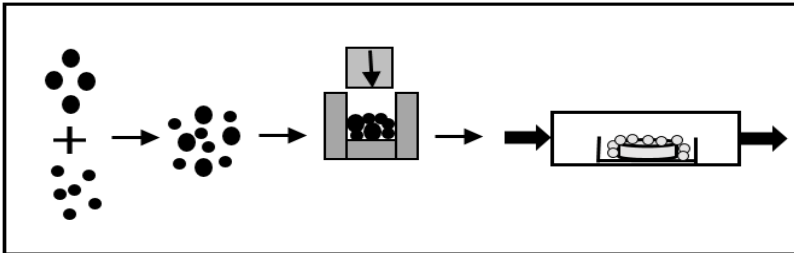


Figure 1: Schematic diagram of PM processing route under argon and reducing environment

Result and Discussion

Phase identification

Figure 2 shows the XRD patterns of TiH₂ powder, Nb powder, and TiNb alloy sintered at 1200°C with the heating rate of 5 °C/min. The XRD patterns attached with the SEM images for each powder and sintered alloy are illustrated in Figure 2. Figure 2 (a) and (b) indicate that the peaks present correspond to TiH₂ and Nb phases, respectively. It can be concluded that the raw powders are pure as there are no peaks that indicate the presence of impurities. In addition, the SEM images displayed in Figure 2 (a) and (b) emphasize the morphology of TiH₂ and Nb powders which are irregular in shape with variety particles size.

Previous research on TiNb alloy mainly emphasized on the correlation between β -phase and Young's modulus value of the alloy. It has been found that greater fraction of β -rich phase resulted in low Young's modulus [12]. As indicated in Figure 2 (c), it was found that the Ti-40Nb alloy consisted of β -phase, α -phase, and Nb. The phases exhibited were supported by XRD result whereby the peaks indicated the presence of each phase respectively. Figure 2 (c) reveals that the alloy is dominated by β -phase which is shows in the spectrum in high intensity, respectively.

In Figure 2 (c), there was apparently Nb particle that incompletely diffuses in Ti matrix. As can be seen in the spectrum, the peak of β -Ti overlapped with Nb peak as compared to the XRD pattern of Nb as presented in Figure 2 (b). The peak reveals the diffusion of Nb into Ti matrix. At the same time, it shows the Nb atom did not completely diffuse in Ti matrix. The apparent of Nb particle was due to its large particles size and inadequate of reaction time. Larger particles with small surface area tend to have less energy and sinter more slowly [19].

There is the presence of α -Ti phase at the sintered sample. The β -phase of Ti (space group *Im3m*) is difficult to retain its phase at room temperature [21]. Upon cooling, this β -phase of Ti transforms into a martensitic which is identical to the low-temperature hexagonal close packed α -Ti phase (space group *P63/mmc*) [14]. Moreover, the XRD result indicates no presence of TiH₂ peak in sintered sample where it can be assumed that the TiH₂ is completely dehydrogenized.

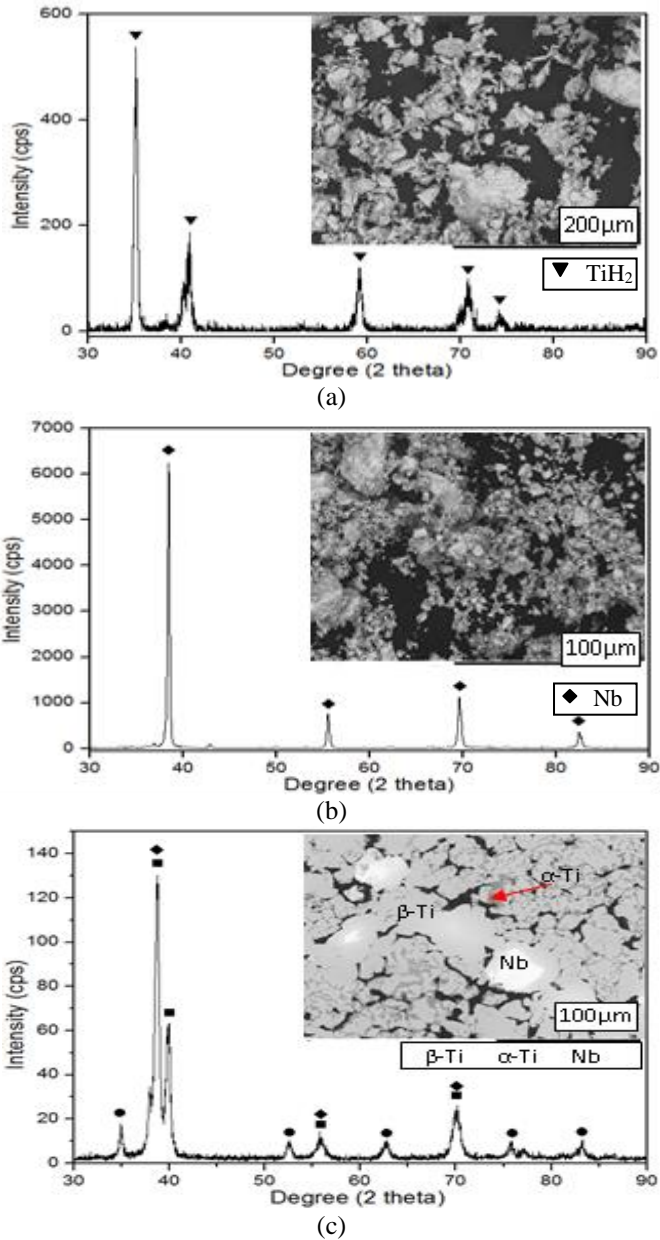


Figure 2: XRD patterns attached with SEM images of: (a) TiH₂ powder, (b) Nb powder, (c) Sintered sample of Ti-40Nb alloy

Porosity and microstructural evolution

Figure 3 shows the porous TiNb alloy fabricated by the present method where apparently it shows an interconnected porous structure with irregular pores size. The percentage of the porosity was $57\% \pm 3$ after calculating it using Equation (1). As indicated in Figure 1, a significant difference is noted where the irregular pore is believed to be attributed from the irregular shape of TiH₂ and Nb powder. It can be seen that the large pores are probably developed from the reaction between dissimilar metal during sintering owing to the different diffusivity of the elements. Meanwhile, the small pore (e.g. Point E) probably generated from the decomposition of TiH₂ as supported by research made by Li et al. [22]. It is reported that, due to decomposition of TiH₂, the NiTi alloy that was fabricated had a greater fraction of small pore, increase pore number and pore distributed more uniform rather than using pure Ti.

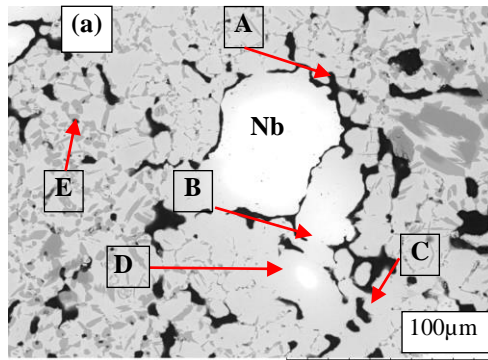


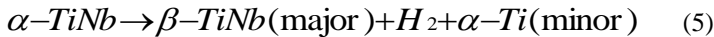
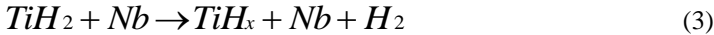
Figure 3: SEM images of sintered sample of TiNb alloy at 1200°C

During sintering of TiNb mixture, several thermal reactions might occur. Ideally, during the sintering process, the TiH₂ will undergo dehydrogenation process where it release H atom and eventually produces new generated Ti atom that is ready for the formation of an alloy. On the other side, the dehydrogenation process occurred at around 450°C [23], thus, it is below the temperature that Ti atom still bonds with H atom. The bonding with H atom prevents the Ti atom from bonding with an oxygen atom. The bonding with H atom will reduce the oxidation process at a low temperature as a concern with high affinity of Ti atom toward oxygen atom at low temperature.

The sintering process was conducted under argon environment in the present work. Hence, this process basically can cause the fresh Ti atom to easily being oxidized. This is the reason why normally Ti-based alloy conducted the sintering process using high vacuum furnace. The oxidation of

Ti can easily occur especially once the Ti atom was generated from the dehydrogenation process of TiH₂ as described in Equation (3) and (4). Both equations illustrate the initial stage formation of TiNb alloy. Concerning the affinity of Ti atom that was easily oxidized, a new approach whereby adding CaH₂ as the wicking agent had been introduced [24]. The general chemical equation of dissociation of CaH₂ into Ca ion and hydrogen gas had been described in detail in Equation (6).

From the Equation (3), (4) and (6), it shows the formation of hydrogen gas at the end of the reaction. The hydrogen gas is basically helping in producing a reducing environment inside the furnace chamber. The reducing environment basically prevents oxidation from occurring by removing oxygen atoms. On the other side, after approximately 770°C, the TiH₂ almost completely undergoes dehydrogenation process as reported by Liu et al. [25]. Since the TiH₂ almost completely undergoes dehydrogenation process, the CaH₂ now takes place of TiH₂ in order to provide a continuous reducing environment in preventing the oxidation process. From Equation (6), it can be noted that the CaH₂ will undergo reduction whereby it produced a reducing environment. The available Ca ion would further undergo oxidations that safeguard the TiNb alloy from being oxidized. The reduction occurred at the decomposition temperature of approximately 799°C.



The pores exhibited in the TiNb alloy are most probably by the formation of the Kirkendall pores and resulted from the growth of the grain boundary. The morphology of Ti-40Nb alloy is depicted in Figure 3 where it can be seen in Point A, the growth of the grain boundary between Nb particle and Ti particles. The pore that has been exhibited remains in the grain boundaries which continually inhibit the grain growth of TiNb alloy. In Point B, it shows Nb is diffused entirely in Ti matrix where the grain boundaries consequently break away from the pores [19]. Considering the particle size of TiH₂ and Nb powders, the particle size of Nb is bigger than TiH₂ powder. Therefore, it can be assumed that the diffusion reaction of Nb atom is slower than Ti atom [18]. Hence, the diffusion of Ti-Ti was dominant in the reaction of the sintered alloy. Equation 5 represents simple understanding on the sintering process of TiNb alloy at the final stage, respectively.

Moreover, at the range temperature of 900°C to 1500°C, the diffusion coefficient of Nb in β -Ti is larger with four to six order of magnitude rather than Ti in Nb matrix [26]. The unbalanced diffusion rate of Ti in Nb and Nb

in Ti causes the formation of Kirkendall pores (e.g. Point C). The mechanism of diffusion which developed a pore is by the vacancy diffusion. Hence, in this present work, the vacancy diffusion mechanism was the one that permitted the formation of pores. The β -phase (e.g Point D) is the evidence of solid state diffusion between the Ti particles and Nb particles.

Mechanical Analysis

The fracture surface of the sintered TiNb alloy was subjected to SEM fractography as shown in Figure 4. The fracture sample indicates brittle sample which is smooth cleavage facets. The fracture might probably be due to porosity and phase presence in the alloy. This is due to crack that is demonstrated by the stress concentration around the pore as presented in Figure 4. As indicated in Table 2, the Young's modulus in the present work was 17 ± 4 GPa while yield strength was 300 ± 6 MPa. This value was compatible with Young's modulus of a human femur.

Comparing with other processing route, the present processing route had lower Young's modulus value and yield strength value that might be probably be due to β -rich phase and a higher number percentage of porosity. The β -phase of Ti was in body centre cubic (BCC) crystal lattice formation while α -phase Ti was in hexagonal closed packed (HCP) crystal structure [21]. The slip system in BCC is higher than HCP structure whereas the slip distance in BCC is lower than HCP crystal lattice. Thus, the BCC structure has a higher tendency to undergo plastic deformation because of dislocation motion that can easily occur. Also, the presence of Nb atom in BCC crystal lattice probably helps in reducing the Young's modulus value. Furthermore, the high value of Young's modulus for other methods was due to the presence of martensitic transformation phase; for instance α' , α'' and ω phase. This phase reduces the slip system of the alloy. Therefore, it becomes difficult to compress the alloy. Thus, results obtained was in high Young's modulus value.

This present research obtains a large number of porosity rather than other methods. It can be assumed that the porosity has significance effect in lowering the Young's modulus value. Meanwhile, in yield strength case, the present work also obtains a low number of yield strength as compared to other method. Even though, it had a low amount of yield strength, it is still higher than the yield strength of the human femur in which further studies need to be attained. The low number of yield strength was due to the presence of large pore size [27].

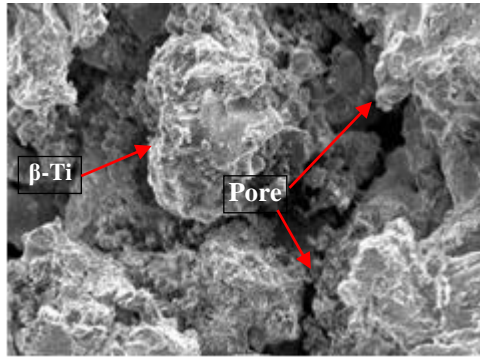


Figure 4: Fracture surfaces of the sintered TiNb alloy

Table 2: The compressive properties of the Ti-40Nb alloy by PM method compared to those of reference Ti-40Nb alloy by another existing method.

	Yield strength (MPa)	Young's Modulus (GPa)	Porosity (%)
Arc melting [14]	~600	57	-
Selective laser melting [15]	968 ± 8	33 ± 2	17 ± 1
Hot pressing [15]	1400 ± 19	77 ± 3	3 ± 2
Powder metallurgy	300 ± 6	17 ± 4	55 ± 3

Conclusion

It has been revealed that it is possible to fabricate Ti-40Nb alloy by using low-cost processing route with porous architecture and β -rich phase. The combination of both properties demonstrated low Young's modulus value of 17±4 GPa with a compatible yield strength of 300±6 MPa. These values are compatible with human femur bone. The TiH₂ gives a beneficial effect on Ti-40Nb alloy as the precursor for Ti atom and as the pore former which resulted in small pore features. The irregular pore structure with a porosity of 55±3% developed might be induced probably from the Kirkendall effect and the grain boundary formation. The diffusion in Ti-40Nb alloy was dominated by Ti-Ti diffusion instead of other diffusion reaction.

The usage of TiH₂ in the fabrication of Ti-40Nb alloy can be further studied in order to know the significant influences on microstructure and mechanical properties of the alloy. These findings can be used to produce a fully β -phase alloy with porous structure for implant material especially for femur bone with the required Young's modulus. The processing route in this

present work might establish a reasonable production route for biomedical TiNb devices owing to low-cost processing route employed.

Acknowledgement

The present work was financially supported by the Ministry of Higher Education (MOHE) under the framework of Research Acculturation Grant Scheme (RAGS) (project code: RAGS/1/2014/TK04/UITM/4). Appreciation and gratitude are also extended to the Research Management Institute of UiTM for facilitating this project.

References

- [1] M. Özcan and C. Hämmerle, "Titanium as a reconstruction and implant material in dentistry: Advantages and pitfalls," *Materials (Basel)*, vol. 5, no. 9, pp. 1528–1545, 2012.
- [2] C. N. Elias, J. H. C. Lima, R. Valiev, and M. a Meyers, "Biomedical Applications of Titanium and its Alloys," *J. Miner. Met. Mater. Soc.*, no. March, pp. 46–49, 2008.
- [3] M. Geetha, A. K. Singh, R. Asokamani, and A. K. Gogia, "Ti based biomaterials, the ultimate choice for orthopaedic implants – A review," *Prog. Mater. Sci.*, vol. 54, no. 3, pp. 397–425, May 2009.
- [4] Z. Esen, E. Tarhan Bor, and Ş. Bor, "Characterization of loose powder sintered porous titanium and Ti6Al4V alloy," *Turkish J. Eng. Environ. Sci.*, vol. 33, no. 3, pp. 207–219, 2009.
- [5] Y. Li, C. Yang, H. Zhao, S. Qu, X. Li, and Y. Li, "New Developments of Ti-Based Alloys for Biomedical Applications," pp. 1709–1800, 2014.
- [6] P. R. Walker, J. LeBlanc, and M. Sikorska, "Effects of aluminum and other cations on the structure of brain and liver chromatin," *Biochemistry*, vol. 28, no. 9, pp. 3911–3915, May 1989.
- [7] M. Abdel-Hady Gepreel and M. Niinomi, "Biocompatibility of Ti-alloys for long-term implantation.," *J. Mech. Behav. Biomed. Mater.*, vol. 20, pp. 407–15, Apr. 2013.
- [8] Y. H. Li, R. B. Chen, G. X. Qi, Z. T. Wang, and Z. Y. Deng, "Powder sintering of porous Ti-15Mo alloy from TiH₂ and Mo powders," *J. Alloys Compd.*, vol. 485, no. 1–2, pp. 215–218, 2009.
- [9] G. Chen, P. Cao, and N. Edmonds, "Porous NiTi alloys produced by press-and-sinter from Ni/Ti and Ni/TiH₂ mixtures," *Mater. Sci. Eng. A*, vol. 582, pp. 117–125, 2013.
- [10] A. Bansiddhi and D. C. Dunand, "Shape-memory NiTi foams produced by replication of NaCl space-holders," *Acta Biomater.*, vol. 4, no. 6, pp. 1996–2007, 2008.

- [11] M. H. Ismail, R. Goodall, H. A. Davies, and I. Todd, "Formation of microporous NiTi by transient liquid phase sintering of elemental powders," *Mater. Sci. Eng. C*, vol. 32, no. 6, pp. 1480–1485, 2012.
- [12] K. Zhuravleva, A. Chivu, A. Teresiak, S. Scudino, M. Calin, L. Schultz, J. Eckert, and a. Gebert, "Porous low modulus Ti40Nb compacts with electrodeposited hydroxyapatite coating for biomedical applications," *Mater. Sci. Eng. C*, vol. 33, no. 4, pp. 2280–2287, 2013.
- [13] J. Davidson and P. Kovacs, "Biocompatible low modulus titanium alloy for medical implants," *US Pat. 5,169,597*, 1992.
- [14] Y.-H. Hon, J.-Y. Wang, and Y.-N. Pan, "Composition/Phase Structure and Properties of Titanium-Niobium Alloys," *Mater. Trans.*, vol. 44, no. 11, pp. 2384–2390, 2003.
- [15] K. Zhuravleva, M. Bönisch, K. Prashanth, U. Hempel, A. Helth, T. Gemming, M. Calin, S. Scudino, L. Schultz, J. Eckert, and A. Gebert, "Production of Porous β -Type Ti–40Nb Alloy for Biomedical Applications: Comparison of Selective Laser Melting and Hot Pressing," *Materials (Basel)*, vol. 6, no. 12, pp. 5700–5712, Dec. 2013.
- [16] M.H. Ismail, Porous NiTi Alloy by Metal Injection Moulding (MIM) using Partly Water Soluble Binder System, Ph.D. thesis, University of Sheffield, 2012
- [17] I. A. Mwamba and L. H. Chown, "The use of titanium hydride in blending and mechanical alloying of Ti-Al alloys," *J. South. African Inst. Min. Metall.*, vol. 111, no. 3, pp. 159–165, 2011.
- [18] D. Zhao, K. Chang, T. Ebel, H. Nie, R. Willumeit, and F. Pyczak, "Sintering behavior and mechanical properties of a metal injection molded Ti–Nb binary alloy as biomaterial," *J. Alloys Compd.*, vol. 640, pp. 393–400, Aug. 2015.
- [19] R. M. German, *Powder Metallurgy and Particulate Materials Processing: The Processes, Materials, Products, Properties and Applications*. Metal Powder Industries Federation, pp. 20-56, 2005.
- [20] A H. Burstein, D. T. Reilly, and M. Martens, "Aging of bone tissue: mechanical properties.," *J. Bone Joint Surg. Am.*, vol. 58, no. 1, pp. 82–86, Jan. 1976.
- [21] L. M. Gammon, R. D. Briggs, J. M. Packard, K. W. Batson, R. Boyer, and C. W. Dombay, "Metallography and Microstructures of Titanium and Its Alloys," vol. 9, 2004.
- [22] B.-Y. Li, L.-J. Rong, and Y.-Y. Li, "The influence of addition of TiH₂ in elemental powder sintering porous Ni–Ti alloys," *Mater. Sci. Eng. A*, vol. 281, no. 1–2, pp. 169–175, 2000.
- [23] D. Mandrino, I. Paulin, and S. D. Škapin, "Scanning electron microscopy, X-ray diffraction and thermal analysis study of the TiH₂ foaming agent," *Mater. Charact.*, vol. 72, pp. 87–93, 2012.

- [24] H. H. Mohd Zaki and J. Abdullah, "Comparison studies on solid state diffusion of Ni-Ti and Ni-TiH₂ under CaH₂ reducing environment," *Mater. Lett.*, vol. 121, pp. 36–39, Apr. 2014.
- [25] H. Liu, P. He, J. C. Feng, and J. Cao, "Kinetic study on nonisothermal dehydrogenation of TiH₂ powders," *Int. J. Hydrogen Energy*, vol. 34, no. 7, pp. 3018–3025, 2009.
- [26] Y. Liu, T. Pan, L. Zhang, D. Yu, and Y. Ge, "Kinetic modeling of diffusion mobilities in bcc Ti-Nb alloys," *J. Alloys Compd.*, vol. 476, no. 1–2, pp. 429–435, 2009.
- [27] K. Ishizaki, S. Komarneni, and M. Nanko, *Porous Materials: Process technology and applications*, vol. 27. Springer Science & Business Media, 2013.